Journal of Great Lakes Research xxx (xxxx) xxx

Contents lists available at ScienceDirect

Journal of Great Lakes Research

journal homepage: www.elsevier.com/locate/jglr

Assessing water clarity status and long-term trends in North America's largest lakes using ESA's Ocean Colour Climate Change Initiative (OC-CCI) products

Caren Binding [a,*,1], Matt Morison [b], Michael Sayers [c], Karl Bosse [c], Xinhua Zhu [d], Chuiqing Zeng [a], Varunan Theenathayalan [a]

[a] Environment and Climate Change Canada, Canada Centre for Inland Waters, 867 Lakeshore Road, Burlington, ON L7S1A1, Canada
[b] Manitoba Environment and Climate Change, 14 Fultz Blvd, Winnipeg, MB R3Y 0L6, Canada
[c] Michigan Tech Research Institute, Michigan Tech University, Ann Arbor, MI, United States
[d] Fisheries and Oceans Canada, Freshwater Institute, 501 University Crescent, Winnipeg, MB R3T 2N6, Canada

ARTICLE INFO

Communicated by Anthony Vodacek

Keywords:
Lake remote sensing
Water clarity
OC-CCI
Secchi

ABSTRACT

Water clarity, as measured by Secchi disk depth (Z_{SD}) or diffuse attenuation (Kd), is an important indicator of a lake's ecosystem state and can be reliably retrieved using satellite remote sensing. By combining data from multiple satellite missions, the European Space Agency's Ocean Colour Climate Change Initiative (OC-CCI) aims to deliver stable, long-term, satellite data products suitable for trend assessments. Here we demonstrate the value of OC-CCI products for reporting on water clarity status and long-term trends in North America's largest lakes. Extensive matchups between the OC-CCI Kd at 490 nm (Kd_{490}) and in situ Z_{SD} observations spanning 25 years enabled robust multi-lake validation of Z_{SD} retrievals over a wide range of water clarity conditions ($R^2 = 0.9$, MAPE = 29.6 %, BIAS = 6.6 %, N = 4297) providing a transferable model for large-scale mapping of inland water clarity. Significant differences in Z_{SD} retrieval uncertainty were observed between years, missions, and specific periods marking changes in the sensor datasets contributing to the OC-CCI products. Bias-correction of the OC-CCI Kd_{490} provided confidence in the assumption of seamless continuity in this multi-mission dataset, thereby allowing long-term time-series analyses. Seasonal, inter-annual and inter-decadal variability and trends in lake-wide average Z_{SD} were subsequently evaluated for nine large lakes across Canada and the U.S. over the 1998–2023 period, capturing the timing and magnitude of significant shifts in water clarity conditions. Observations agree well with documented periods of ecosystem change in response to the cumulative impacts from harmful algal blooms, nutrient status, invasive species, and hydrological events.

1. Introduction

North America's inland freshwater systems are of enormous socio-economic importance, providing vital drinking, industrial and recreational water resources, supporting valuable ecosystem services, contributing to global biogeochemical cycling, and serving as sentinels of anthropogenic influence on aquatic environments. Water quality, as defined by its chemical, physical, and biological characteristics, plays a critical role in determining the beneficial uses of these water resources. A key visual indicator of water quality, water clarity is often integral to inland and coastal water quality monitoring programs and reporting by governing agencies (Keith et al., 2023). Typically measured as a Secchi disk depth (Z_{SD}) or diffuse attenuation coefficient (Kd), water clarity is an important gauge of ecosystem health state, while also playing a central role in regulating pelagic and benthic primary productivity, energy and material transfer, and impacting a waterbody's aesthetic value. Freshwater quality varies regionally across North America and is affected by human disturbances such as land-use and climate change (Huot et al., 2019; Deutsch et al., 2022). Shifts in long-term climate trends, such as increasing water temperatures (Tong et al., 2023) and

* Corresponding author.
E-mail address: caren.binding@ec.gc.ca (C. Binding).
[1] Given her role as Editor, Caren Binding had no involvement in the peer-review of this article and has no access to information regarding its peer-review. Full responsibility for the editorial process for this article was delegated to Anthony Vodacek.

https://doi.org/10.1016/j.jglr.2024.102454
Received 18 July 2024; Accepted 29 September 2024

decreasing ice cover (Huang et al., 2022), are having widespread impacts on these freshwater systems, with high-latitude regions in particular experiencing rapid transformations (Ruhland et al., 2023). Increases in terrestrially-derived dissolved organic matter (DOM) leading to the browning of inland waters (Williamson et al., 2015), eutrophication and resulting nuisance or harmful algal blooms (HABs) (Stumpf et al., 2012; Binding et al., 2019), non-native invasive species (Barbiero and Tuchman, 2004), and the impact of changing hydrology and magnitude of flooding events on runoff and erosion, have led to notable changes in lake water clarity.

Consistent, long-term records of lake water quality are therefore critical not only for effective management of water resources but for understanding current and future responses of freshwater systems to anthropogenic change. However, data scarcity remains a pressing challenge, with spatially and temporally representative in situ data being prohibitively expensive and logistically challenging to obtain. For example, in Canada's two northern great lakes, Great Slave Lake and Great Bear Lake, relatively few studies and little historical limnological data exist; remote access and a harsh subarctic climate make continuous monitoring datasets rare, yielding spatially patchy and temporally limited data sets (Muir et al., 2013). Even in the relatively data-rich Laurentian Great Lakes, sparse spatial coverage and the intermittent nature of ground-based monitoring often preclude robust conclusions regarding long-term lake-wide water quality status and trends (Dove and Chapra, 2015). The frequency, geographic coverage, and accessibility of satellite Earth Observation (EO) data therefore provide an ideal solution for long-term, large-scale monitoring of water quality.

Several satellite ocean colour missions with water quality observation capabilities have been in operation over the last few decades (e.g., SeaWiFS, MODIS, MERIS, VIIRS, OLCI), forming an invaluable contiguous record of aquatic colour radiometry data since 1997. Each satellite mission, however, has a finite lifespan (~10 years), resulting in long-term datasets being pieced together with observations from multiple sensor-specific archives. Challenges exist, therefore, in seamlessly merging products to produce consistent multi-mission remote sensing products for time-series analyses, due to the need to combine datasets from satellite missions with significant differences in sensor and product characteristics. Inconsistencies in the spectral, spatial, and temporal resolutions of remote sensing platforms mean that products require continuity assessment before such multi-sensor datasets can be relied upon. Otherwise, the potential for artifacts propagated into downstream products may ultimately affect the conclusions drawn from a time-series analysis (Groom et al., 2019; Mélin et al., 2017). Various methods exist for creating merged multi-mission ocean colour records (IOCCG, 2007) and several initiatives make global merged data products routinely available to users (e.g. GlobColor, OC-CCI). The European Space Agency's (ESA) Climate Change Initiative Ocean Colour (OC-CCI) products aim to deliver stable, long-term, satellite-based Essential Climate Variable (ECV) data suitable for trend assessments (Sathyendranath et al., 2019). The distributed OC-CCI products include spectral remote sensing reflectance (Rrs(λ)), and derived optical and biogeochemical properties including absorption (a), backscatter (b_b), downwelling attenuation coefficient at 490 nm (Kd_{490}) and chlorophyll-a.

Numerous approaches exist for estimating Z_{SD} from Rrs, ranging from empirical algorithms based on single band reflectance (Binding et al., 2007; Binding et al., 2015) or band ratios (Olmanson et al., 2008; Deutsch et al., 2022), analytical solutions based on radiative transfer theory (Lee et al., 2018), and more recently machine learning approaches (Maciel et al., 2023; Zhang et al., 2022). Binding et al. (2007; 2015) used a simple empirical relation between Z_{SD} and Rrs at 555 nm (Rrs_{555}) from three sensors (CZCS, SeaWiFS and MODIS), capturing dramatic changes in water clarity across the Laurentian Great Lakes resulting from oligotrophication, regional HABs, and changing biogeochemical processes influencing whiting events. Although this previously applied empirical relationship appears robust in the predominantly scattering waters of the Laurentian Great Lakes, Binding et al. (2015) noted the same approach may not be appropriate in strongly absorbing waters, thereby limiting the algorithm's suitability across wide-ranging optical water types. Considering the optical complexity of lake waters and the variable relationship between Z_{SD} and the optically active parameters contributing to water clarity (Jiang et al., 2019), here we extend and modify our previous work using a robust semi-analytical Kd_{490} algorithm accounting for absorption and scattering properties. The OC-CCI Kd_{490} is computed using the model of Lee et al. (2005) after applying the Quasi-Analytical Algorithm (QAA, v.6, Lee 2014) to derive a(λ) and b_b(λ) by inverting Rrs(λ). Because it resolves the effects of both absorption and scattering on water clarity, the QAA approach is anticipated to be more representative of the wide-ranging optical water types across North America's inland waters, thereby offering the potential for a more transferable model for large-scale mapping of water clarity compared with simple empirical approaches based on reflectance alone.

In this study, we aim to demonstrate the value of ESA's OC-CCI Kd_{490} products for reporting on the long-term temporal variability of water clarity in North America's largest lakes. The assumption of seamless continuity in the OC-CCI Kd_{490} multi-mission product is critical in allowing long-term water clarity trend assessments. Despite the increasing availability of high-fidelity in situ optical property datasets in recent years (e.g. Lehmann et al., 2023), however, few large-scale datasets of Kd_{490} exist dating back to the beginning of the OC-CCI time series in the late 1990s. In this study we therefore made use of extensive historical in situ Z_{SD} datasets curated from Canadian and U.S. water quality monitoring programs to calibrate a Z_{SD} retrieval algorithm from the OC-CCI Kd_{490}. Multi-mission continuity of the derived OC-CCI Z_{SD} product was assessed before analyzing seasonal, interannual, and decadal status and trends in lake water clarity.

2. Methods

2.1. Study areas

North America's nine largest lakes were selected for this study (Fig. 1). Their surface areas range from the smallest Lake Athabasca at 7,500 km^2 to Lake Superior at 82,000 km^2. The lakes span in location latitudinally from 43° to 68° N and longitudinally from 75° to 125° W, covering wide-ranging climates and ecozones. The Laurentian Great Lakes have seen notable fluctuations in water clarity in recent decades (Binding et al., 2015, 2007) brought about by the combined effects of excessive nutrient loading and resulting HABs (Watson et al., 2016), subsequent nutrient management (Dove and Chapra, 2015), invasive zebra mussels (Fahnenstiel et al., 2010; Klerks et al., 1996), whiting events (Watkins et al., 2013), periodic sediment resuspension and shoreline erosion. Lakes Superior, Michigan, Huron, and Ontario are typically considered oligotrophic with high water clarity in their offshore waters and regional nearshore turbidity, whereas Lake Erie displays a distinct gradient from a shallow turbid and eutrophic western basin which experiences annual cyanobacterial blooms (Binding et al., 2019; Stumpf et al., 2012), to deeper and meso/oligotrophic central and eastern basins.

Lake Winnipeg, located within the Canadian province of Manitoba, is the 10th largest freshwater lake in the world covering a surface area of 23,750 km^2. A shallow prairie lake, it is characterized by low water clarity brought about by high concentrations of dissolved organic matter and mineral resuspension as well as recurring severe cyanobacteria blooms (Binding et al., 2018). Lake Winnipeg has experienced a zebra mussel invasion initially identified in 2013 (DFO, 2014), colonizing most of the available hard substrate in the south basin and Narrows regions by 2017–19 (Depew et al., 2021). North-west of Lake Winnipeg and on the boundary of the Canadian provinces of Alberta and Saskatchewan is Lake Athabasca, which is 283 km long with a maximum width of 50 km. Fed from the southwest by the Peace and Athabasca rivers, the western arm of Lake Athabasca is an area of active sediment deposition resulting in strong turbidity gradients from west to east

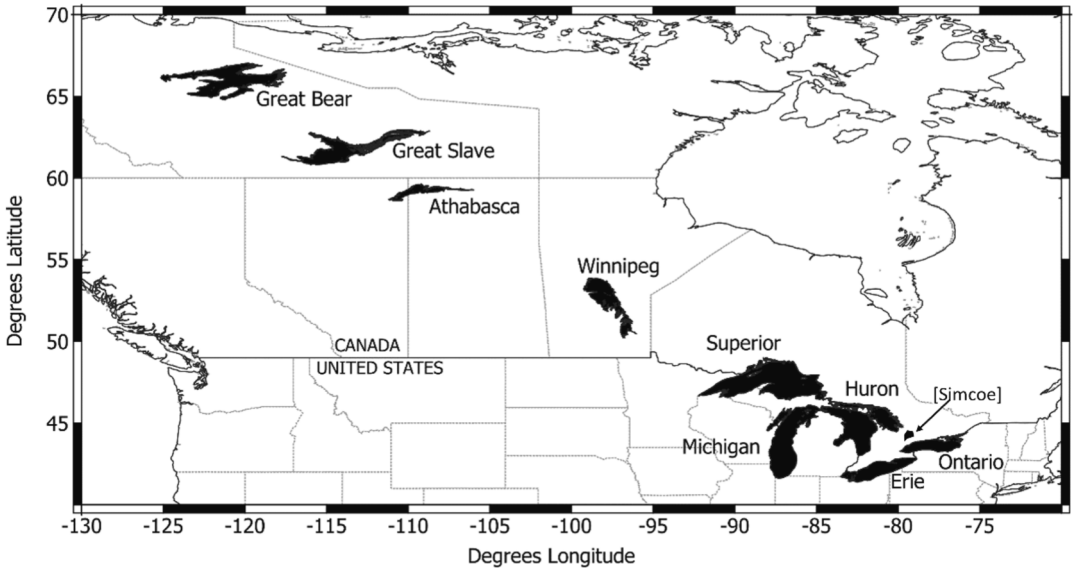

Fig. 1. Analysis focused on nine of the largest lakes by area in Canada and the U.S., including the Laurentian Great Lakes, Lake Winnipeg, Lake Athabasca, Great Slave, and Great Bear Lakes. In situ data from Lake Simcoe was also included in the matchup-exercise.

(Evans, 2000). At its outlet, the Slave River flows northward to Great Slave Lake in the Northwest Territories. Great Slave Lake is the deepest subarctic lake in North America and the second largest lake (after Great Bear Lake) that is entirely within Canada. It is seasonally ice-covered and typically oligotrophic, waters are generally clear in the east arm and turbid in the shallower Resolution Bay where the Slave River contributes an extensive plume of suspended sediments (Ruhland et al., 2023; Evans, 2000). Finally, Great Bear Lake, also in the Northwest Territories, is the northernmost of the lakes studied. At its outlet, the Great Bear River flows west into the Mackenzie River. Great Bear Lake is a deep, cold monomictic lake (Johnson, 1975) and is typically ice-covered from late November to July (Rao et al., 2012). Its watershed is small and relatively undeveloped and as such the lake is considered a pristine ecosystem, with oligotrophic waters of high water clarity (Evans, 2000).

2.2. Datasets

2.2.1. OC-CCI Kd_{490}

OC-CCI produces a multi-mission record of Rrs using data from the following sensors: SeaWiFS (Sea-viewing Wide-Field-of-view Sensor; September 1997 to December 2010), MERIS (MEdium spectral Resolution Imaging Spectrometer; April 2002 to April 2012), MODIS-Aqua (Moderate-resolution Imaging Spectroradiometer; July 2002 to December 2019), VIIRS (Visible and Infrared Imaging Radiometer Suite, October 2011 to 2019), and OLCI (Ocean Land Colour Instrument; OLCI-A May 2016 to present, and OLCI-B June 2018 to present). Level-1 data from each sensor are atmospherically corrected to level-2 Rrs using either POLYMER or SeaDAS l2gen (for SeaWiFS) and binned to 4 km (sinusoidal grid) level-3 products with BEAM/SNAP (ESA/ESRIN, 2022). Mixed pixels in the nearshore were removed by masking. The spectral wavebands of SeaWiFS, MODIS, and VIIRS are band shifted to the core reference bands of MERIS (412, 443, 490, 510, 560, 665 nm) by computing the Inherent Optical Properties (IOPs) using the QAA of Lee et al. (2002) as updated in v.6 (Lee, 2014) and back-computing the Rrs bands using a high-resolution spectral model (ESA/ESRIN, 2022). OLCI requires no band-shifting due to its consistent bands with the legacy MERIS bands. SeaWiFS and MODIS Rrs are further corrected to remove biases relative to MERIS Rrs, as calculated on a per-pixel basis over the 2003–2007 period when all sensors overlapped. VIIRS and OLCI are then also bias-corrected using their coincident periods with MODIS. Finally, overlapping sensor data are merged by simple averaging. As a water turbidity indicator distributed by the OC-CCI, Kd_{490} is derived with the model of Lee et al. (2005) using the $a(\lambda)$ and $b_b(\lambda)$ coefficients from QAA and the solar-zenith angle as inputs (Jerlov, 1976), with b_{bw} coefficients from Zhang et al. (2009). Daily and monthly composite Kd_{490} products (v. 6.0) were accessed through the OC-CCI web portal (https://www.oceancolour.org/portal). Monthly lake-average Kd_{490} were retrieved for each of the nine lakes in Fig. 1, using shapefiles of the lake boundaries obtained from the HydroLAKES database (Messager et al., 2016).

2.2.2. In situ Secchi disk depth (Z_{SD}) matchups

In situ measures of Z_{SD} are typically conducted using a 20 cm black-and-white Secchi disk lowered into the water over the shaded side of a research/monitoring vessel or other platform, with the depth at which the disk remains visible to the naked eye being recorded. An extensive dataset of historical in situ Z_{SD} (>10,000 observations) was curated from several bi-national research and monitoring programs. Environment Climate Change Canada's (ECCC) Watershed Hydrology and Ecology Research Division (WHERD) has conducted regular research cruises in the lower Great Lakes (Erie and Ontario) since 2004 for the collection of aquatic optics, remote sensing, and biogeochemical variables, typically targeting peak algal bloom occurrences in August/September. In addition, ECCC's Freshwater Quality Monitoring and Surveillance (FWQMS) program operates regular spring and summer whole-lake surveys of water quality on Lakes Ontario, Erie, Huron, and Superior, data from which can be readily accessed in the government of Canada's open data catalogue. Similarly, the U.S. Environmental Protection Agency (EPA) Great Lakes National Program Office (GLNPO) samples water quality variables to assess the health of the Great Lakes ecosystem, with data housed in the Great Lakes Environmental Database (GLENDA).

The U.S. National Oceanic and Atmospheric Administration (NOAA) Great Lakes Environmental Research Laboratory (GLERL), along with the Cooperative Institute for Great Lakes Research (CIGLR), created a HAB monitoring program for western Lake Erie that has conducted routine sampling of the basin since 2012 (Boegehold et al., 2023). Sampling takes place throughout the pre-bloom, bloom, and post-bloom period (typically from May through October) at eight stations which were chosen to reflect a broad range of environmental conditions. The monitoring program consists of many parameters including biogeochemistry (e.g., chlorophyll-a, nutrients, toxins) and optical properties for the calibration and validation of remote sensing algorithms.

Since 2011, a group of arctic aquatic researchers from the Department of Fisheries and Oceans Canada implemented a cumulative impact monitoring program in the main basin of Great Slave Lake, under the funding support of the Northwest Territories (NWT-CIMP). A 245-grid system, separated by 5 min of latitude and 10 min of longitude, was developed to cover the six management areas of the main basin of Great Slave Lake (Zhu et al., 2024; Zhu et al., 2017). Sampling occurred between June and August 2012–2022 and included measures of the limnological variables: depth (m), temperature (°C), dissolved oxygen (mg/l), pH, turbidity (NTU), conductivity (µs/cm) and Z_{SD} (m).

Manitoba Environment and Climate Change (MECC) has maintained a long-term water quality monitoring program on Lake Winnipeg since 1999 to track changes in lake water quality over a network of 65 stations ranging across the North and South basins of the lake and extending radially from near-shore to off-shore/lake centre. Chemical and biological samples are collected during the spring, summer, and fall lake cruises from the Lake Winnipeg Research Consortium Inc.(LWRC)-operated Motor Vessel Namao. LWRC, MECC, and ECCC also collect physiochemical parameters coincident with water and sediment sample collection, including Z_{SD}.

We also included in the matchup analysis Z_{SD} data from Ontario's provincial monitoring program on Lake Simcoe. Although Lake Simcoe was not considered further in the analysis of Z_{SD} status and trends due to its smaller lake area, data from its centre-lake monitoring station provided an extensive long-term dataset of in situ Z_{SD} spanning the whole period of the OC-CCI and therefore was a valuable additional dataset for assessing the continuity of the Kd_{490} products. No in situ data was acquired from Lake Athabasca or Great Bear Lake, but the comprehensive range of observations collected across the other lakes (capturing oligotrophic, eutrophic, dystrophic, and turbid waters) is expected to adequately capture the variability of conditions in these two large lake systems given what is known about their general water quality status.

Station coordinates and sampling dates from the compiled dataset of in situ Z_{SD} observations were uploaded to the OC-CCI data portal to extract same-day single pixel (at 4 km resolution) matchups of OC-CCI satellite-derived Kd_{490}. In total 4297 matchups were obtained across all lakes, with Lake Erie and Lake Winnipeg offering the highest number of matchups, and Great Slave Lake the least (Fig. 2a). Fig. 2a documents the natural range of water clarity conditions on the nine lakes, with Lake Winnipeg by far the most turbid, and Lakes Huron, Superior and Michigan exhibiting the clearest waters. The full range of matchup observations spanned Z_{SD} from 0.2 m to 36 m, with 29 % of the matchups representing highly turbid waters in which $Z_{SD} < 2$ m (Fig. 2b). Total matchups in any given year ranged from 82 to 274, except for 2020 due to the impact of the COVID-19 pandemic on sampling campaigns that year (Fig. 2c). The gradual increase in monitoring effort over the time period is notable, with the last few years' decline attributed both to remnant impacts of the pandemic on monitoring programs, and normal delays in releasing data to the public domain.

2.3. Data analyses

The relationship between OC-CCI Kd_{490} and in situ Z_{SD} was assessed using leave-one-year-out cross-validation. The slope and intercept of linear least-square regressions were determined sequentially on data subsets after leaving one year out (Electronic Supplementary Material (ESM) Table S1). The predictive performance of each relationship was then assessed on the independent remaining year's data, calculating the MAPE and BIAS according to Eq (1) and Eq (2) every year from 1998 to 2022 (i.e. matchups from 1998 were used to assess the performance of

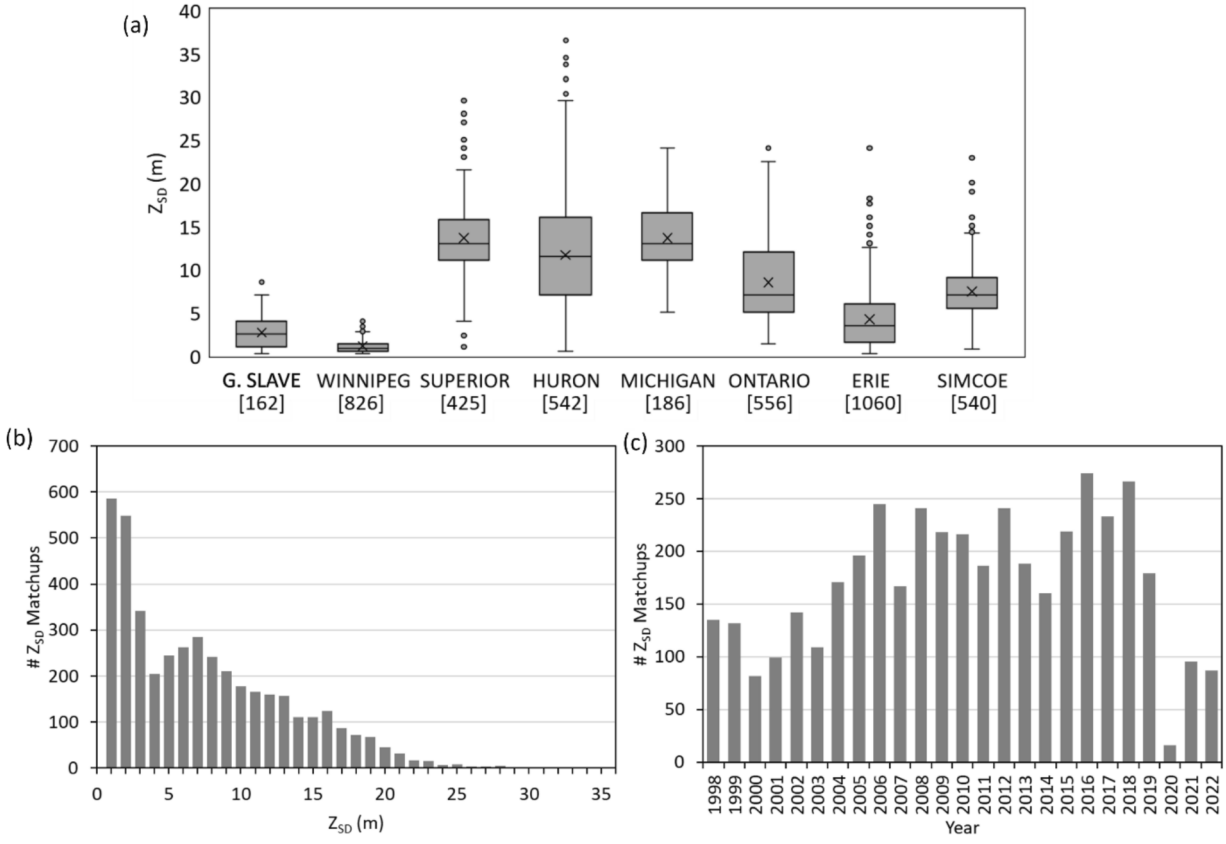

Fig. 2. (a) Boxplot distribution of in situ Z_{SD} for each lake used in the matchup dataset, where the box captures the 1st to 3rd quartiles, the median is marked by the horizontal line, mean marked by a cross, and whiskers extend to mark the minimum and maximum. [N] is the total number of matchups for each lake, (b) number of Z_{SD} matchups per 1 m bin in the range 0–36 m, and (c) total Z_{SD} matchups per year.

the relationship generated with data from 1999 to 2022, those from 1999 validated the relationship from 1998 and 2000–2022, etc.). The final linear relationship between Kd_{490} and Z_{SD}, along with its performance metrics, were taken as the average of all subset assessments.

$$MAPE = \frac{100}{n}\sum_{i=1}^{n}\left|\frac{Z_{SD}(Pred)_i - Z_{SD}(Obs)_i}{Z_{SD}(Obs)_i}\right| \quad (1)$$

$$BIAS = \frac{100}{n}\sum_{i=1}^{n}\left(\frac{Z_{SD}(Pred)_i - Z_{SD}(Obs)_i}{Z_{SD}(Obs)_i}\right) \quad (2)$$

In order to assess inter-annual and inter-sensor continuity in the OC-CCI products, the final single Kd_{490}-Z_{SD} relationship was applied to all matchups and the MAPE and BIAS of predicted Z_{SD} calculated. Mood's median test (Mood, 1950) was then used to assess whether there were any significant differences in the median MAPE and BIAS of each year, mission, and key periods of changing data sources in the OC-CCI dataset. If there was significant evidence that population medians were different, post hoc testing was conducted to determine the magnitude of the differences using pairwise Mood's median tests with pairwise bootstrap confidence intervals, correcting for multiple simultaneous inferences by applying a Bonferroni correction.

To view seasonal and interannual variability in the OC-CCI lake-wide average Z_{SD}, monthly and annual Z_{SD} anomalies (ΔZ_{SD}, Eq (3)) were determined as the percentage difference between the annual (or monthly) average Z_{SD} and the long term (1998–2023) average Z_{SD}. Annual averages were calculated as the average of all available monthly Z_{SD}, which varied for each lake due to data gaps brought about by seasonal ice extent, but were kept consistent for all years on each lake. For most lakes the annual Z_{SD} included observations for May-November, whereas for the northernmost lakes, winter ice cover reduced the observation window to June-October for Great Slave Lake and Lake Athabasca, and July–September for Great Bear Lake.

$$\Delta Z_{SD} = 100\left[\frac{Z_{SDi} - \left(\frac{1}{n}\sum_{i=1998}^{2023} Z_{SDi}\right)}{\left(\frac{1}{n}\sum_{i=1998}^{2023} Z_{SDi}\right)}\right] \quad (3)$$

Where Z_{SDi} is either the annual or monthly average Z_{SD}.

Nonparametric Mann–Kendall tests for monotonic trends were applied (Hussain and Mahmud, 2019) to determine the significance of temporal Z_{SD} trends using moving windows of ten years, with the magnitude of those temporal trends estimated using Thiel–Sen's slope (m_{TS}). These tests are recognized to be robust to outliers and more accurate for skewed or heteroskedastic data and have been used widely for assessing temporal trends in limnological studies (Ho et al., 2019; Taranu et al., 2015; Hirsch et al., 1982).

3. Results

3.1. Z_{SD} Calibration-Validation

The total 4297 matchups resulted in a robust relationship between in situ Z_{SD} and the OC-CCI Kd_{490} (Fig. 3) with average retrieval uncertainties of 29.6 % MAPE and 6.6 % BIAS based on the leave-one-year-out cross-validation (ESM Table S1). Individual lake data contributions occupied different spaces in this relationship due to the inherent differences in their range of water clarity conditions (Fig. 4). Leave-one-lake-out cross-validation therefore resulted in small deviations in the slope of the relationship between Z_{SD} and Kd_{490}, although MAPE and BIAS remained in the 29–32 % and 0–15 % ranges respectively. Furthermore, no more than 10 % of any individual lake data fell outside the 99 % prediction interval of the relationship from the remaining lake data, suggesting that despite some expected regional differences, the average relationship has broad applicability and adequately represents the Z_{SD}-Kd_{490} relationship for all the validated lakes in the study.

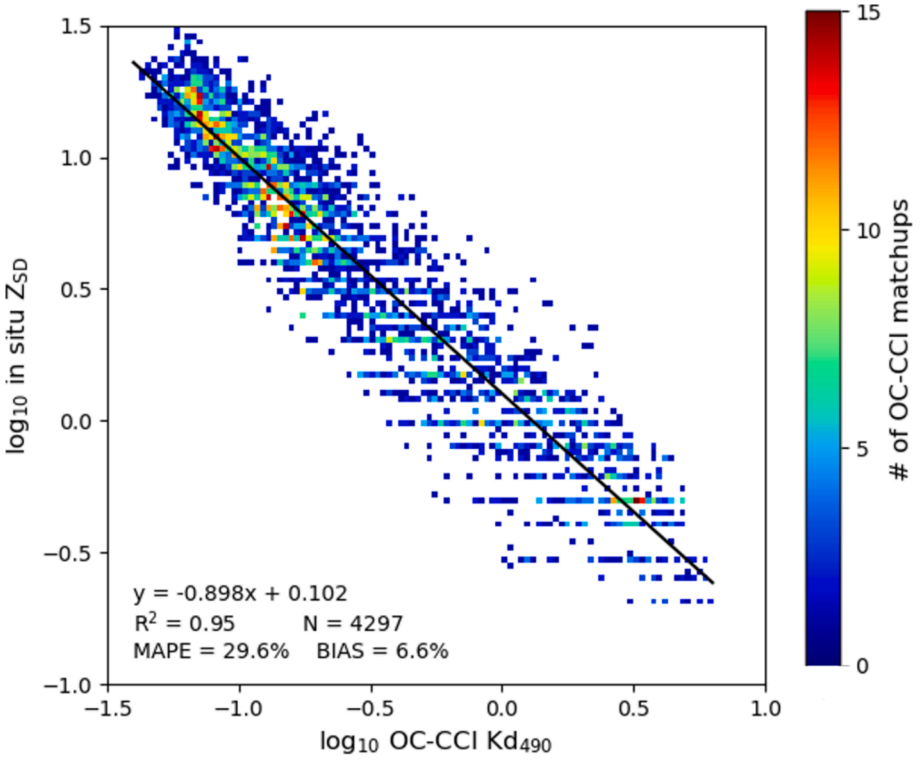

Fig. 3. Agreement between same-day matchups of in situ Z_{SD} and the satellite-derived daily OC-CCI Kd_{490} product for the entire multi-lake multi-mission dataset.

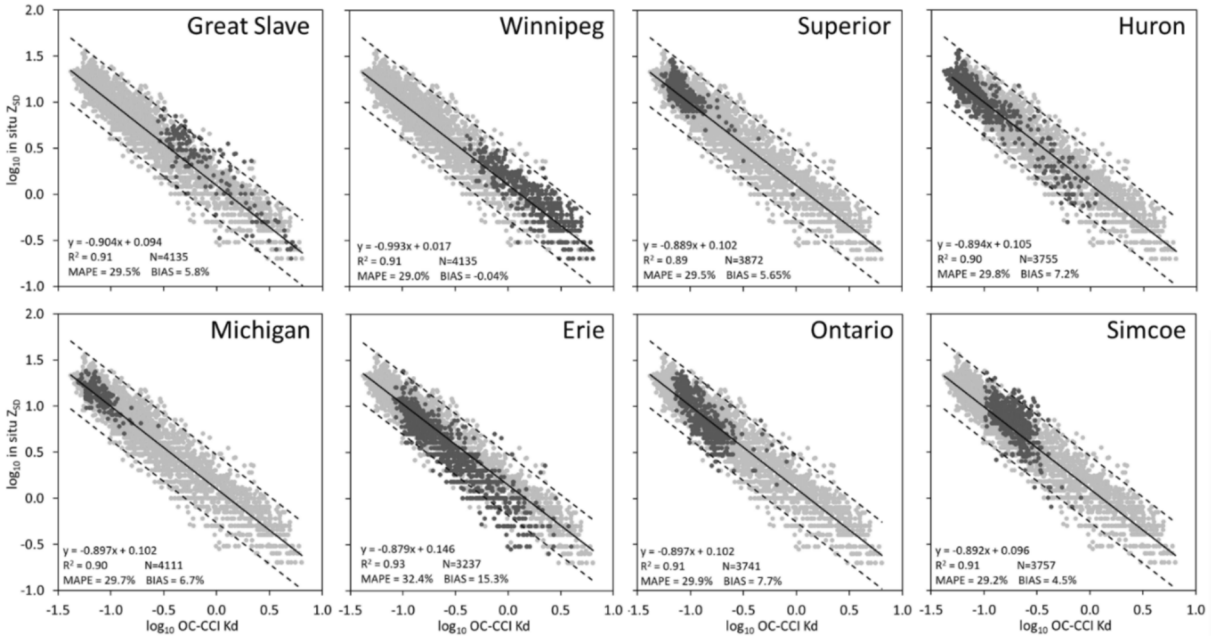

Fig. 4. Lake-specific distribution of data in the $\log_{10}$ Z_{SD} vs $\log_{10}$ OC-CCI Kd_{490} space. Centre line represents the algorithm fit from the leave-one-lake-out validation (i.e. using all data except the left-out lake, N is therefore the total dataset minus the data from the named lake), dashed lines represent the 99 % confidence interval of that fit.

3.2. Multi-Sensor continuity assessment

Adequate numbers of matchups for each year of the time series (with the exception perhaps of 2020 due to pandemic-related impacts on monitoring programs) allowed reliable estimates of annual Z_{SD} retrieval uncertainties. Assessment was then made of the temporal consistency in retrieval uncertainties as reported by %MAPE and %BIAS. Annual median MAPE and BIAS ranged from 15.5 to 35.6 % and from −25 to 23.3 % respectively over the 1998–2022 time-period (Fig. 5). Significant differences were found among the reported annual median MAPE (Moods median $\chi^2 = 113.94$, $p < 0.0001$) and BIAS (Moods Median $\chi^2 = 220.04$, $p < 0.0001$).

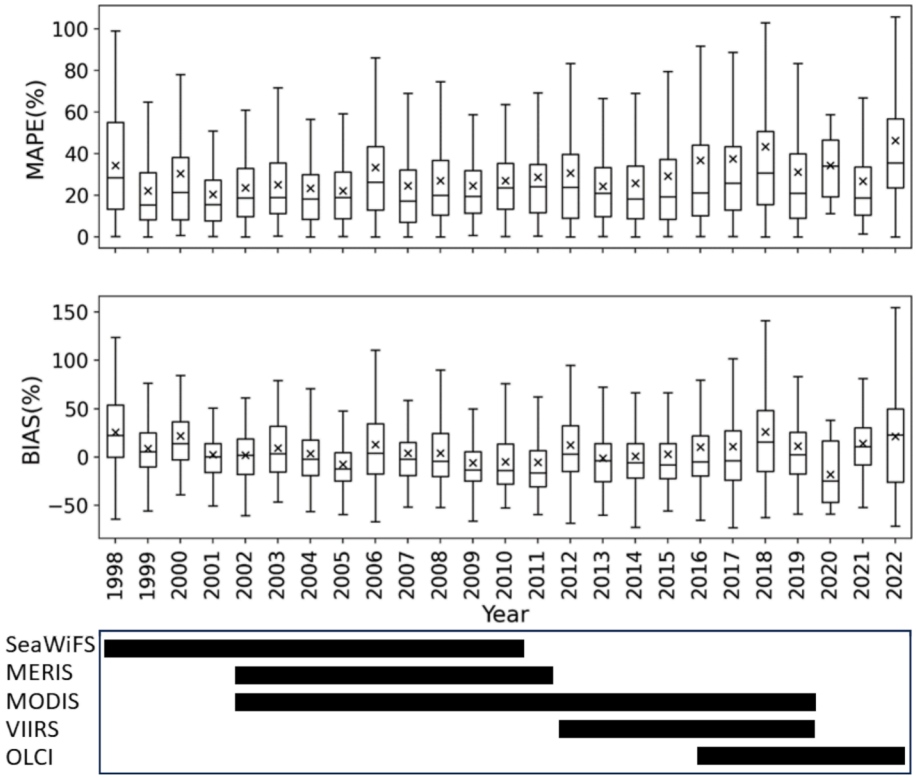

Fig. 5. Time series of annual Z_{SD} retrieval MAPE (a) and BIAS (b), using the best-fit relation of the whole dataset as reported in Fig. 3. For reference, the lower panel (c) captures the periods of the five contributing sensor datasets.

Similarly, the retrieval uncertainties were calculated for key periods across the dataset to ascertain any mission-related offsets that could lead to artifacts in the time-series. Firstly, uncertainties were calculated for the independent mission periods, 1998–2010 for SeaWiFS, 2002–2011 for MERIS, 2002–2019 for MODIS, 2015–2019 for VIIRS and 2016 to present for OLCI (Fig. 5c). Median MAPE in retrieved Z_{SD} for any given mission period ranged from 20 % to 25.2 %, with the highest uncertainty recorded during the VIIRS and OLCI windows. Moods median tests confirmed significant differences in the median MAPE between missions ($\chi^2 = 32.6564$, $p < 0.0001$), with OLCI noted as having higher retrieval uncertainties than SeaWiFS (by 5.3 %, $p < 0.0001$), MERIS (by 4.5 %, $p = 0.0001$), and MODIS (by 3.8 %, $p = 0.0017$). Median BIAS ranged from an underestimate of Z_{SD} by 6.5 % for MERIS to an overestimate of 2.8 % by OLCI, again with significant differences among mission periods ($\chi^2 = 40.9011$, $p < 0.0001$). Due to the overlap in mission operating periods and the range of data contributions to the composite dataset, however, it is challenging to identify and correct mission-specific artifacts using these windows. Instead, following the approach of Oostende et al. (2022) a second assessment was carried out for key periods of change in the data sources; the time-series was divided into four broad sub-periods defined as the period when only SeaWiFS was available (P1: 1998–2002), the period when MERIS and MODIS were incorporated (P2: 2002–2011), the period when VIIRS was launched and MERIS terminated (P3: 2012–2015) and the period when OLCI was included (P4: 2016 − present). For these defined periods, median MAPE ranged from 18.3 % for P1 to 24.0 % for P4, with significant differences reported among the groups ($\chi^2 = 16.16$, $p = 0.0011$) which was attributed to the difference between P4 and P1 (5.6 %, $p = 0.004$) and between P4 and P2 (3.3 %, $p = 0.004$). Likewise, the median BIAS in retrieved Z_{SD} was 9.4 % for P1, −6.5 % for P2, −3.4 % for P3 and 1.5 % for P4, with significant differences noted between P1 and all other periods as well as between P2 and P4. It was these period-specific median biases that were subsequently applied to the time-series of OC-CCI Z_{SD} as a correction to remove potential artifacts in the dataset introduced by sensor merging.

3.3. Inter-annual Z_{SD} variability and trends

The Z_{SD} retrieval algorithm in Fig. 3 was applied to monthly composite OC-CCI-Kd_{490} products, corrected for the period-specific bias from Fig. 5b, and extracted as lake-wide average Z_{SD} for each lake from 1998 to 2023. Derived monthly Z_{SD}, annual Z_{SD} anomalies, decadal trends, and rates of change are presented in Fig. 7 for each of the nine lakes. Of the northern lakes, Great Bear Lake was the clearest, with monthly lake-average Z_{SD} ranging from 6.1 m to 9.7 m, and with little interannual variability in the annual average Z_{SD}, deviating from the long-term average by a maximum of 10.4 % in 2014 and −9.2 % in 2006. Nevertheless, significant decadal trends in Z_{SD} were observed, declining over 1998–2007, before a period of increasing Z_{SD} through 2015, followed by declines until 2023. Great Slave Lake exhibited much lower water clarity, ranging from a minimum lake-average Z_{SD} of 0.7 m to a maximum of only 2.1 m and with significant interannual variability, with annual Z_{SD} deviating from the long-term average by as much as 39 % in 2010 and −36 % in 2020. Interdecadal trends captured a period of increasing Z_{SD} until ~ 2010 before declining. Similarly, Lake Athabasca's monthly lake-average Z_{SD} ranged from 0.8 m to a maximum of 3 m. Its peak annual Z_{SD} deviated from the long-term average by 42 % in 2015, and like Great Slave Lake, saw a minimum Z_{SD} (30 % below normal) in 2020. There were no significant decadal trends before 2005, after which there were three decadal periods of increasing Z_{SD} before declines driven by the low of 2020. Lake Winnipeg showed the lowest water clarity of all the lakes studied, ranging from a minimum monthly lake-average Z_{SD} of 0.3 m to a maximum of only 1.4 m. Below-average annual water clarity (by as much as 24 %) persisted for over a decade before transitioning abruptly in 2012 to a period of elevated Z_{SD}, peaking in 2021 at 32 % above the long-term average. Decadal trends confirm significant declines in Lake Winnipeg water clarity until ~ 2009 then switching to a period of significantly increasing Z_{SD} before stabilizing in the last few years. However, the absolute rate of decadal change in Z_{SD} (Fig. 7d) peaked at only 2.3 cm per year due to the low baseline

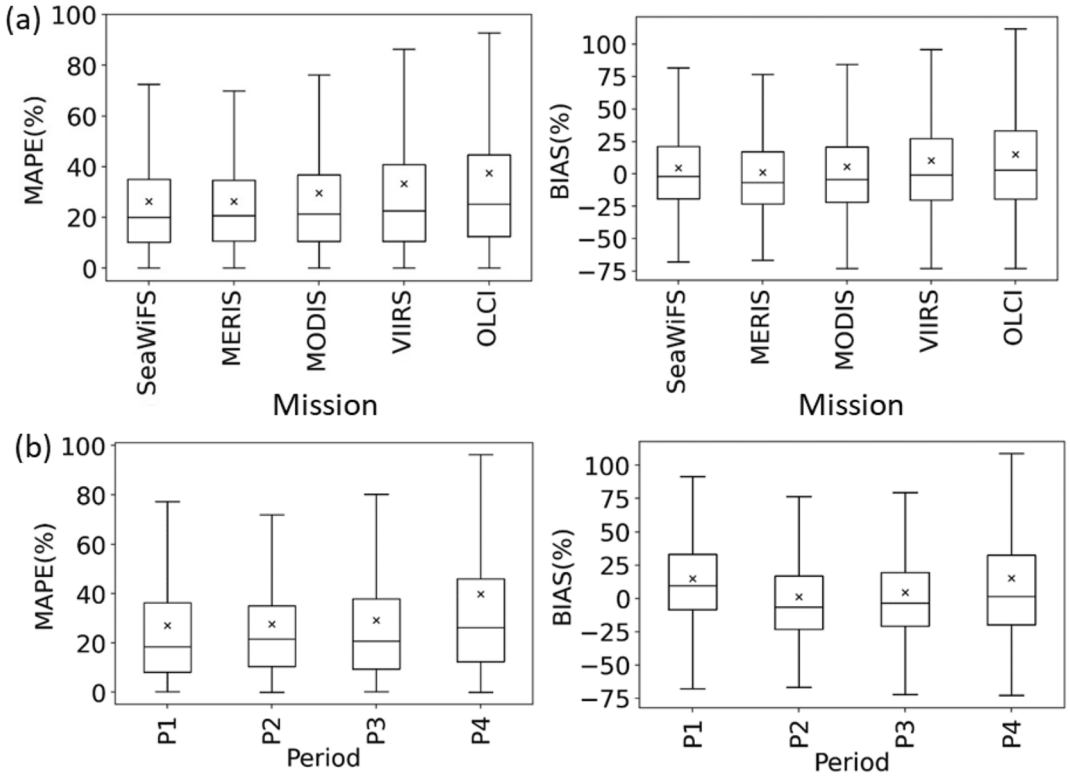

Fig. 6. Z_{SD} retrieval MAPE and BIAS using the best-fit relation of the whole dataset as reported in Fig. 3, for (a) mission-specific periods and (b) time periods representing key changes in the input data sources of the OC-CCCI as defined by P1−P4.

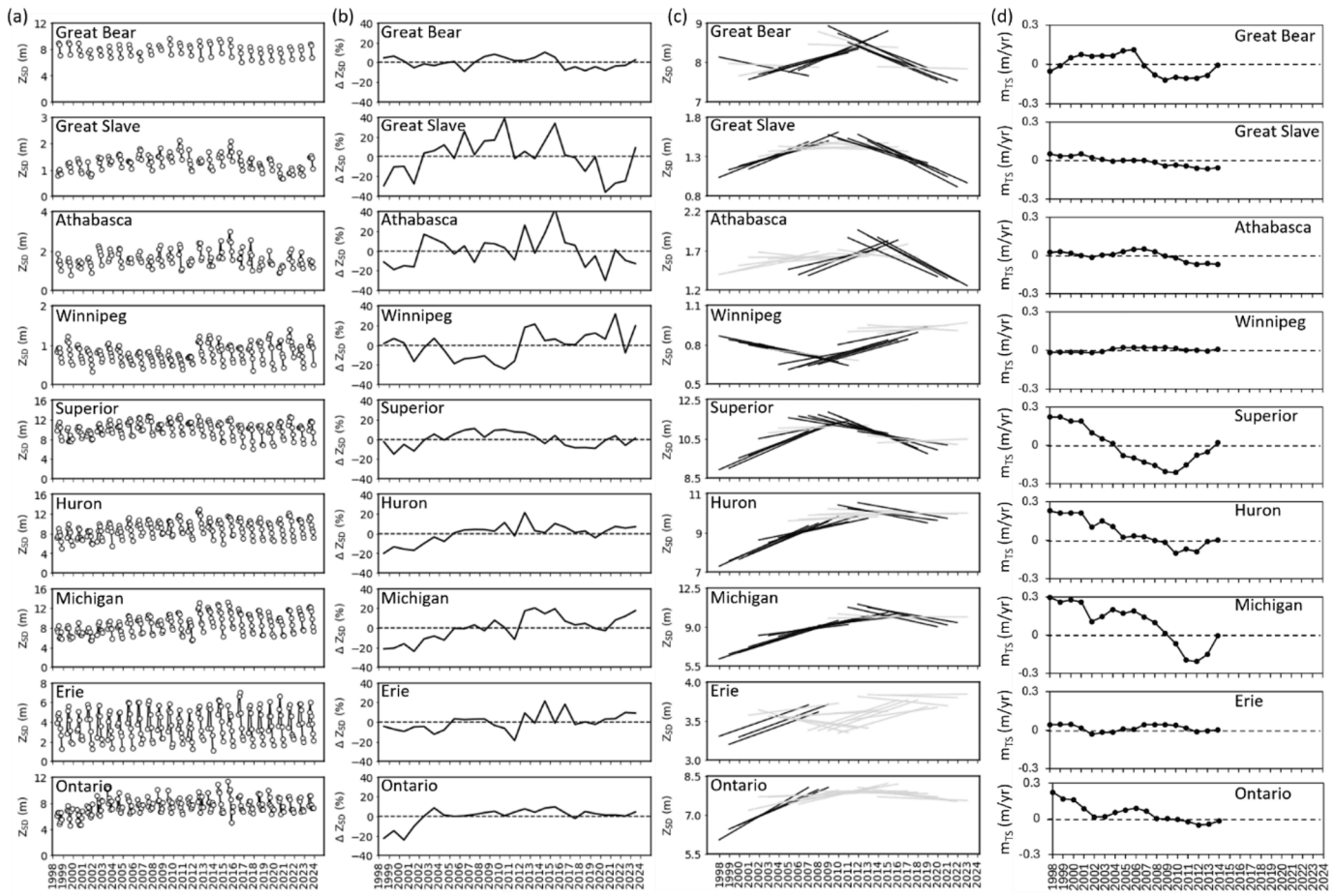

Fig. 7. Time series of (a) OC-CCI derived monthly lake-average BIAS-corrected Z_{SD}, (b) annual Z_{SD} anomaly as the percentage difference between the annual average Z_{SD} and the long term average Z_{SD} (1998–2023), (c) 10 year rolling trends in Z_{SD} from Theil-Sen's Slope after Seasonal Mann-Kendall test for monotonic trends (grey = insignificant trend, black = significant trend at $p < 0.05$), and (d) the magnitude of the Thiel Sen slope (m_{TS}) for each decadal interval plotted on the first year of each 10 year period, where positive slopes above the dash line indicate a trend of increasing Z_{SD} and negative slopes below the dash line indicate a trend of decreasing Z_{SD}.

levels of clarity on the lake.

Of the Laurentian Great Lakes, Lake Superior has some of the highest water clarity, with lake-average monthly Z_{SD} ranging from 6.1 m to 12.9 m. Minimum annual Z_{SD} was observed in 1999 (15.1 % below average), with an increasing trend toward peak Z_{SD} in 2007 (at 11 % above average), before significant declines since ~ 2009. Annual rates of change in Z_{SD} (m_{TS}) ranged from 22 cm per year for the decade beginning in 1998 to −21 cm per year for the decade beginning 2010. Lake Huron showed a lower minimum water clarity than Superior (monthly minimum of 5.1 m observed in 1998), but at its peak, had a higher Z_{SD} than Superior (peaking at 13 m in 2012). Decadal trends showed a consistent increase in Z_{SD} from the 1990 s through to ~ 2011 at a rate of 21–23 cm per year before stabilizing. Lake Michigan shows very similar water clarity conditions to Lake Huron, with a range in monthly Z_{SD} of 5.5–13.3 m and a consistent trend of increasing water clarity from a minimum in the 1990s to a peak around 2012–15, increasing at a rate of up to 30 cm per year. Lake Erie is the shallowest and thus most turbid of the Laurentian Great Lakes, with monthly Z_{SD} ranging from 1.1 m to 7.0 m. There was little significant change in Z_{SD} recorded in Lake Erie with the exception of a small increase captured over the first three decadal periods. Finally on Lake Ontario, monthly Z_{SD} ranged from 4.5 m to 11.4 m, with a notable period of below-average water clarity from 1998 to 2002 before significant increases to fairly stable conditions for the remainder of the time series.

3.4. Z_{SD} seasonality

Seasonality of water clarity showed significant variation between lakes and over time (Fig. 8). On Great Bear Lake, where observations were restricted to just July-September, there was limited seasonal variability both within and between years. Water clarity peaked in July, declining through August and September. Despite interannual variability in monthly Z_{SD} of less than +/-10 %, seasonal decadal trends suggest significant recent declines in September water clarity (ESM Figure S1). In Great Slave Lake the minimum annual Z_{SD} observed in 2020 was driven by low water clarity across the whole season, with August and September in particular being 47 % and 48 % below normal respectively. Seasonality of low water clarity decades (e.g. those starting in 2013 and 2014) showed a notable decrease in Z_{SD} in July, increasing in August before declining into the fall. In contrast, the seasonality of higher water clarity decades (e.g. those starting in 2006 and 2008) showed a broader spring/summer peak. Of note, monthly Z_{SD} in July 2010 and August 2015 was more than 60 % and 54 % above seasonal norms respectively. In Lake Athabasca, Z_{SD} peaked consistently in August, reaching a minimum Z_{SD} in October. The 1998–2007 decade exhibited the lowest water clarity, whereas the highest water clarity was observed in the 2007–2016 and 2008–2017 decades. Lake Winnipeg saw significant declines in June-September Z_{SD} until ~ 2012 (ESM Figure S1), with summer Z_{SD} of 2010 being 30 % below the long-term average, leading to a minimum decadal Z_{SD} in the 2002–2012 period. This then shifted to increasing spring and summer Z_{SD}, with peak

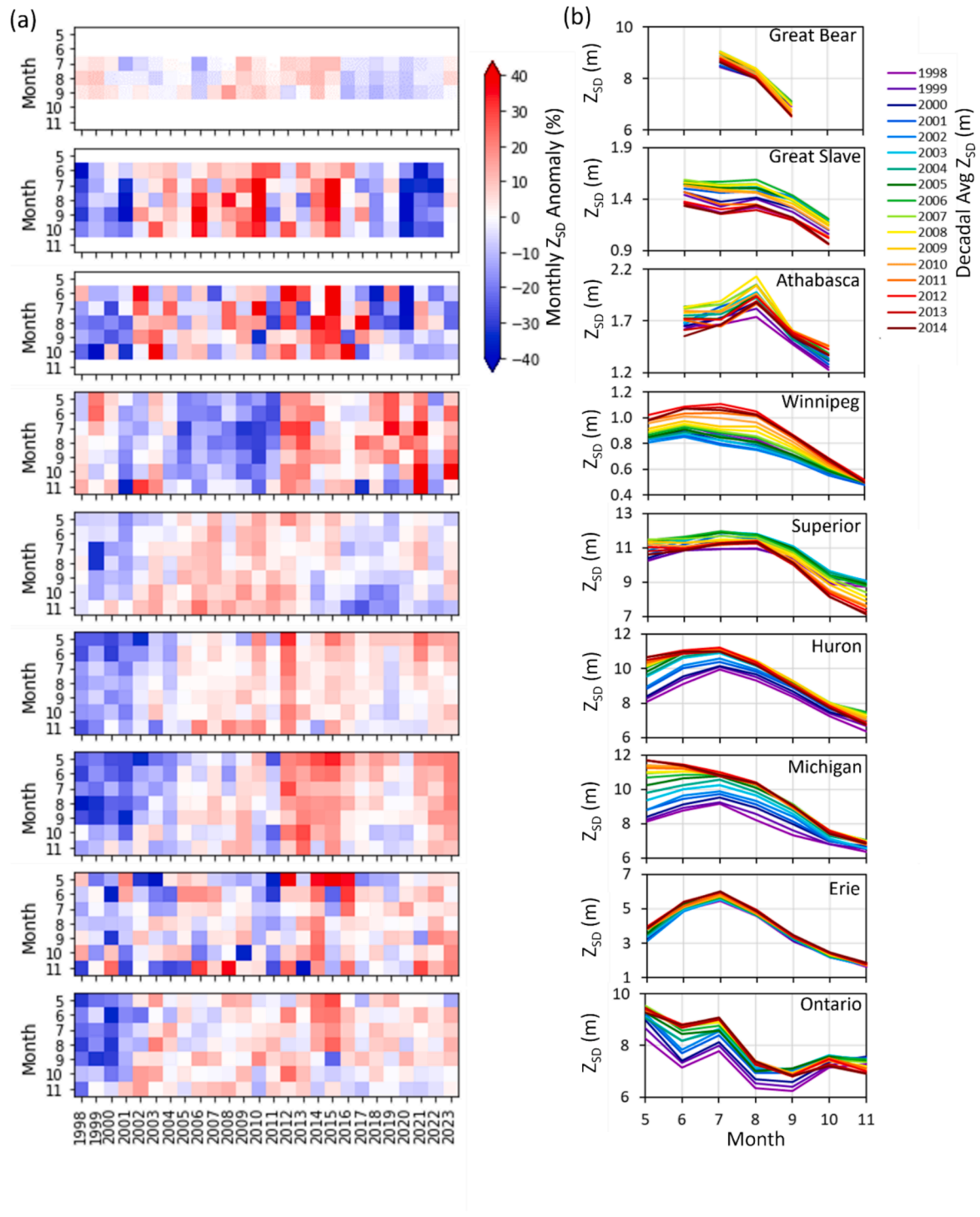

Fig. 8. (a) Hovmöller diagrams showing monthly Z_{SD} anomalies calculated as the percentage difference between monthly Z_{SD} and the long term (1998–2023) average monthly Z_{SD}, and (b) seasonal variability of decadal average Z_{SD} (i.e. 1998 shows the average monthly Z_{SD} over the 1998–2007 period, 1999 is for 1999–2008, etc).

decadal Z_{SD} in 2012–2022. The greatest interannual variability in monthly Z_{SD} was observed in July. No significant changes in November water clarity were observed, but the decadal seasonality shows some suggestion of the seasonal peak in Z_{SD} broadening or shifting later in the year. The apparent increase in Z_{SD} seasonality on Lake Winnipeg is captured by an increase in the coefficient of variation (CV) of monthly Z_{SD} each year, ranging from 12-27 % before 2012 to 20–37 % after 2012.

The trends that were evident on Lake Superior on an annual basis are mirrored in the monthly Z_{SD}, with increases in Z_{SD} prior to 2012 dominated by increases in spring and summer Z_{SD}. In contrast, declines in more recent years have been more prominent in October and November, with November 2016 and 2017 in particular being 20 % and 26 % below long-term norms respectively. Peak decadal Z_{SD} on Superior was observed in 2003–2012. Lake Huron water clarity typically peaked in July before declining consistently in later months. Lake Huron's spring water clarity saw especially significant increases (ESM Figure S1) ranging from lows of as much as 33 % below normal in May/June prior to 2002 to a peak in 2012 at 32 % above normal, with decadal averages

stabilizing in more recent years.

Very clear shifts in seasonal water clarity conditions were observed in Lake Michigan, with a 44 % increase in decade-average May Z_{SD} from 8.1 m in 1998–2007 to nearly 11.7 m in 2014–2023. Increases over the same period of 33 % and 18 % were recorded for decade-averaged June and July Z_{SD} respectively. Individual monthly anomalies ranged from 37 % below the long-term average in August of 1998 to 33 % above average in May of 2015. Decadal trends captured significant increases for May-August, with no significant trends observed in October and November water clarity (ESM Figure S1). These spring-weighted increases in water clarity have resulted in a shift in the observed seasonal pattern of Z_{SD} on the lake, from a July peak in water clarity in the 1998–2007 period to a May peak in more recent years. The increased Z_{SD} seasonality gained by the higher springtime water clarity is reflected in the average annual CV of 15 % before 2008 increasing to 20 % after 2008.

For the lower Great Lakes, two very different patterns in water clarity seasonality were evident. In Lake Erie, decade-average Z_{SD} peaked consistently in July, reaching a minimum Z_{SD} in November. There's a large amount of interannual variability in monthly Z_{SD} particularly in May (monthly anomalies ranging from −38 % in 2003 to 60 % in 2015) and November (from −38 % in 2015 to 36 % in 2008). Nevertheless, decadal seasonality has remained remarkably stable over the observation period, with no notable monthly trends detected (ESM Figure S2). In contrast, Lake Ontario saw significant increases in Z_{SD} from May through August until around 2008 before stabilizing. The seasonality is driven by peak water clarity in May followed by a local minimum in June, a second peak in July and then the lowest water clarity in August and September before increasing again into October/November. The greatest increase in monthly decade-average Z_{SD} was observed in June, increasing by 23 % from 7.2 m in 1998 to 8.8 m in 2012.

4. Discussion

4.1. Drivers of water clarity changes

Seasonal, inter-annual and inter-decadal variability and trends in Z_{SD} agree well with documented periods of change on each lake in response to the cumulative impacts on water clarity from harmful algal blooms, nutrient status, invasive species, and extreme hydrological events. For example, the time-series captures the impact of an unprecedented high-water year for Great Slave Lake in 2020 (Fig. 7b, Fig. 8a), after precipitation in the watershed reached a 20-year peak. Turbidity subsequently reached historic highs in July 2020 due to very heavy sediment loads from the Slave River, the largest tributary to the lake, gaining much media attention (Cabin Radio, 2020; CBC, 2020) and visible in satellite imagery as an extensive turbidity plume (USGS, 2020). High flows in the Slave River were matched by very high flows in the Peace and Athabasca Rivers, as well as extremely high water levels in the Peace-Athabasca Delta and Lake Athabasca, therefore the low water clarity seen in Great Slave was also mirrored in Lake Athabasca during the same period (Fig. 7b). In contrast, periods of low discharge from the Slave River (e.g. 2005, as observed in ECCC hydrometric data) saw some of the highest water clarity in both Great Slave and Lake Athabasca. In addition to these hydrological drivers, significant changes in biological productivity in these northern lakes have been recently documented (Ruhland et al., 2023; Sayers et al., 2020) which could contribute to the observed seasonal and temporal trends in water clarity. Remote sensing data from 2003 to 2018 (Sayers et al., 2020) showed a steady and significant increase in lake-wide primary production on Great Slave and Great Bear lakes, while pronounced shifts in phytoplankton community composition in response to accelerated Arctic warming have also been documented (Ruhland et al. 2023). The reduced seasonal data availability of the OC-CCI dataset in these northern lakes (from July to September for Great Bear and June to October for Great Slave and Lake Athabasca) highlight some of the limitations of remote sensing of water quality at high latitudes due to ice cover and low solar angles.

Results for Lake Winnipeg suggest a period of declining water clarity followed by a shift to increasing water clarity in recent years beginning in ~ 2012 (Fig. 7b). Since the 1990s, Lake Winnipeg experienced a period of rapid eutrophication, leading to severe recurring algal blooms (Binding et al., 2018; Bunting et al., 2016). Efforts to reduce nutrient loading to Lake Winnipeg are ongoing, with the long-term goal of reducing phosphorus concentrations in the lake to pre-1990 levels (Bunting et al., 2016; Government of Manitoba, 2020). Between 2010 and 2023, implemented management actions prevented an estimated 390 tons of phosphorus from reaching Lake Winnipeg (ECCC, 2024). Total Phosphorus and Nitrogen concentrations in the north basin of the lake were reported to be below the long-term mean in 2012–2019 and 2012–2021 respectively (Government of Manitoba, 2023). Over the same period, invasive zebra mussels (*Dreissena polymorpha*) were introduced to the lake, with the first adult mussels reported in 2013, although anecdotal evidence suggests their arrival may have already occurred in 2012 or earlier (Page, 2020). The establishment of zebra mussels in the Laurentian Great Lakes contributed to significant localized increases in water transparency in the years immediately following their colonization (Holland, 1993). The timing of an apparent regime shift in water clarity conditions on Lake Winnipeg around 2012 toward increasing Z_{SD} is therefore in good agreement with the anticipated dual impacts of implemented nutrient management practices and the introduction of zebra mussels. Further, similarly to Great Slave Lake, annual hydrological variability in sediment loading from relatively TSS-rich tributaries to Lake Winnipeg (Government of Manitoba, 2023) may contribute to annual and longer-term clarity trends and variability.

Increases in water clarity in Lakes Huron, Michigan, and Ontario, particularly in the spring (Fig. 8b), are in good agreement with documented reductions in productivity in those lakes due to the effects of nutrient management and invasive zebra mussels (Barbiero et al., 2012; Evans et al., 2011). Lakes Huron and Michigan have undergone gradual oligotrophication coincident with, and anticipated by, nutrient management implementation (Evans et al., 2011). Barbiero et al. (2012) noted a distinct convergence of the trophic state in the three upper lakes, corroborated here with the increases in transparency in Lakes Huron and Michigan to Secchi depths roughly equivalent to, and sometimes exceeding, Lake Superior (Fig. 7a). Barbiero et al. (2012) also reported that the seasonality of chlorophyll-a has been dramatically reduced in Lake Huron and Lake Michigan, with the spring bloom largely absent from both lakes and instead a seasonal maximum occurring in autumn, as is the case in Lake Superior. These shifts in seasonality have been captured in the decadal trends in water clarity reported here (Fig. 8b). The timing of dramatic drops in production has been found to coincide with the expansion of populations of invasive dreissenid mussels in Lakes Huron and Michigan in the early 2000s and mid-2000s respectively (Evans et al., 2011). In Lake Michigan, adult quagga mussels increased dramatically in density between 2001 and 2006, with extraordinary increases in water transparency along with simultaneous decreases of chlorophyll-a in the late-winter bloom (Kerfoot et al., 2010). Consistent with those observations, here we found the maximum rates of change in Z_{SD} were the decades centered on 2002 through to 2004, with the annual rates of change as high as 30 cm for Lake Michigan and 22 cm for Huron. Lake Huron saw the first switch from below-average summer water clarity to above-average in 2004, whereas Michigan was two years later in 2006 (Fig. 8a).

Lake Erie has undergone a period of re-eutrophication since the mid-1990s, with a resurgence of annual algal blooms persisting mainly in the western basin throughout the summer and into late fall (Scavia et al., 2014; Stumpf et al., 2012; Watson et al., 2016). The blooms of 2011 and 2015 in particular were the largest in the last two decades (Zeng and Binding, 2021) and here results showed June-October average Z_{SD} 14 % and 11 % below normal in those two years, respectively. The lack of any discernible seasonal, interannual or decadal trends in water clarity on Lake Erie is therefore contrary to concerns over the increasing severity of

these blooms. The shallowest of the Great Lakes, Erie also experiences frequent wind-driven resuspension events that often dominate lake-wide water clarity, and it is perhaps this seasonal and interannual variability in mineral turbidity that obscures any potential trends in algal-driven water clarity. Likewise, the blooms in Erie are generally restricted to its western basin, and so reporting here on the whole lake-average Z_{SD} could potentially reduce such spatial heterogeneity.

On Lake Ontario, Barbiero et al. (2006) reported a near doubling of summer Secchi depths in the 1990s, postulating a reduction in calcite precipitation (whiting events), resulting from the effects of dreissenids on offshore calcium concentrations. Satellite-derived Secchi on the lower Great Lakes reported by Binding et al. (2007) suggested a decrease in whiting events and associated water clarity on Lake Ontario between the CZCS and SeaWiFS missions periods, although intermittent whiting events remained. Watkins et al. (2013) showed ongoing whiting events in their time series of Rrs_{550} extending to 2011, and the present study suggests those whiting events remain a frequent contributor to seasonal water clarity, resulting in minima in Z_{SD} in August/September each year. Results here suggest that the previously reported increases in water clarity in Lake Ontario continued into the early 2000s before stabilizing (Fig. 7b). Changes in seasonal Z_{SD} in Lake Ontario were greatest in the spring and early summer (Fig. 8b), corroborating the observations of Binding et al. (2007) which captured dramatic increases in springtime water clarity between CZCS and SeaWiFS, and in agreement with reported reductions in chlorophyll-a following mussel colonization and reductions in total phosphorus to the lake (Nicholls, 2001).

4.2. Multi-mission continuity of the OC-CCI products

The OC-CCI project aims to deliver a consistent and homogenous data set of ocean colour and bio-geo-optical products for long term time-series and climate related studies. While every effort has been made by the OC-CCI team to remove bias and minimize the difference between mission periods, some product uncertainties and discontinuity inevitably remain and user caution is advised particularly around the start and end times of the individual sensor datasets (ESA/ESRIN, 2022). Mélin et al. (2017) assessed temporal trends among the OC-CCI chlorophyll-a products and found overall good agreement between single mission and the merged data products. Nezlin et al. (in review) reported consistency in the timing of chlorophyll-a regime shifts in the Laurentian Great Lakes measured from the OC-CCI dataset compared with those measured from individual sensors, suggesting limited impact of multi-mission data merging on their analysis. However, others have noted significant inter-mission inconsistencies, typically appearing as steps in the OC-CCI products coinciding with mission periods, which could be potentially misinterpreted as natural variability and trends (van Oostende et al., 2022). In the present study, to mitigate the impact of any remaining sensor-specific artifacts in the data, we applied a correction based on the observed interannual variability of Z_{SD} retrieval bias, as determined for the four key periods of data transition in the OC-CCI dataset (Fig. 6b). Even though a large quantity of matchups were available for this exercise, differences in the number (and location) of matchups between years and sensor-specific periods may introduce uncertainty in the applied bias corrections. Other approaches have also been suggested in the literature, for example van Oostende et al. (2022) introduced the temporal gap detection method, to improve the temporal homogeneity of multi-mission datasets by correcting the differences in observational gaps per pixel. Despite these added steps being taken to minimize the uncertainty of inter-sensor bias it cannot be discounted that some discontinuities in the time-series remain. However, the fact that the interannual variability and trends in Z_{SD} presented here varied so distinctly between the lakes studied suggests there were no consistent data-related artifacts overriding our results. Furthermore, the timing of observed changes in Z_{SD} were entirely consistent with known ecosystem shifts and hydrological events in each lake, suggesting that any remaining uncertainty in multi-mission continuity is small and that the OC-CCI captured accurately the temporal variability of water clarity on these lakes.

4.3. Consistency with previous studies

Binding et al. (2015) applied a simple empirical Z_{SD} algorithm built on coincident in situ Z_{SD} and satellite-measured Rrs_{555}, reporting dramatic changes in water clarity of the Laurentian Great Lakes over three mission periods (CZCS, SeaWiFS and MODIS). We would expect the relationship between Z_{SD} and Rrs_{555}, however, to be sensitive to the level of absorption within the waterbody under consideration. We have observed that the algorithm fails in strongly absorbing waters such as black water events in Lake Winnipeg (unpublished work), where the absorption-diminished Rrs_{555} results in significant overestimates in retrieved Z_{SD}. Here we compared the results of the OC-CCI Kd_{490}-derived Z_{SD} with retrievals using the previous Rrs_{555}-based algorithm for the Laurentian Great Lakes (Fig. 9). A good agreement exists between the two approaches for the more turbid waters of Lake Erie and Ontario where algal blooms, sediment resuspension, and whiting events drive water clarity. In contrast, in the clear waters of Lake Superior, Huron and Michigan, the Rrs_{555}-derived Z_{SD} is significantly lower than the OC-

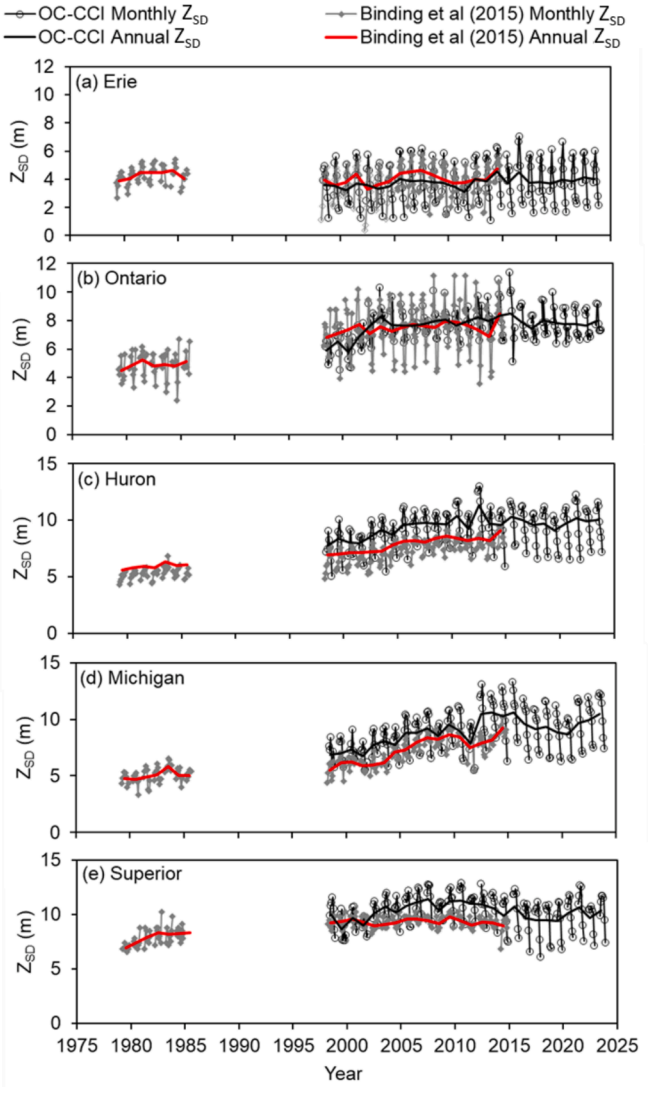

Fig. 9. Time series of lake-wide average Z_{SD} for the Canadian Great lakes derived from the empirical relationship with Rrs_{555} published in Binding et al. (2015) and that validated in the present study from the OC-CCI Kd_{490} product.

CCI derived Z_{SD}. This is consistent with the anticipated effect of absorbing waters on the algorithm calibration in Binding et al. (2015), forcing a higher intercept and therefore resulting in underestimation of Z_{SD} in clear waters, and overestimation of Z_{SD} in strongly absorbing waters (see ESM Figure S2). These results point to an increased confidence in IOP-derived water clarity products relative to simple reflectance-based algorithms, with results of the present study being more broadly applicable over wide-ranging optical water types.

4.4. Variability of the Z_{SD}-Kd_{490} relationship

The OC-CCI project provides ocean colour ECV data products, with a focus on Case-1 water algorithm approaches. Multiple sources of potential variability and uncertainty exist in the distributed Kd_{490} products, particularly for coastal and inland water applications. In addition to the multi-mission merging bias already discussed, further sources of uncertainty in the Kd_{490} products can be attributed to uncertainties in atmospheric correction over optically complex inland waters, regional and temporal variability in the inherent optical properties, contamination from optically shallow waters (i.e. bottom effects) and adjacency effects. Any bias in the retrieved Kd_{490} in these optically complex waters will therefore be propagated into the defined relationship between Kd_{490} and Z_{SD}, which will also include uncertainties brought about by sub-pixel variability, and bias in the inherently subjective measurement of Z_{SD} in the field. Some variability in the Z_{SD}-Kd_{490} relationship can likely be attributed to the coarse spatial resolution of the Level-3 OC-CCI products (4 km), particularly in dynamic nearshore environments. A stronger relationship may be anticipated using the same Kd_{490} products at the sensor's native resolutions. In the past decades, a number of empirical relationships have been developed between Z_{SD} and K_{PAR} or $Kd_{(\lambda)}$ with measurements from various water bodies (Lee et al., 2018). From theory, Z_{SD} can be approximated by $1.48/K_{PAR}$, consistent with the range of coefficients reported in the literature between 1.27 and 2 from in situ datasets (Lee et al., 2018). The equivalent coefficient observed in the present study is 1.19 for the whole multi-lake dataset, so at the low end of the coefficients curated in Lee et al. (2018) but close to those reported for the most turbid waters of Chesapeake Bay (Gallegos et al., 1990). Atmospheric correction in highly turbid waters very often over-corrects reflectance in the blue portion of the spectrum, leading to overestimates in derived Kd_{490}, which may contribute to the low coefficient observed here. Furthermore, the relationships in Lee et al. (2018) are for broad-spectrum K_{PAR} rather than the Kd_{490} reported by OC-CCI. The relationships between water clarity and optically active parameters are complex and variable (Jiang et al., 2019), with different wavelengths sensitive to different water constituents, which can lead to underestimation or overestimation of Z_{SD} for different optical waters from a single relationship (Zhang et al., 2022). Some have proposed a pre-classification step in Z_{SD} retrieval algorithms, for example Liu et al. (2013) categorized waters into three types before establishing empirical relationships, which may provide further improvements in retrieval uncertainties in future efforts. Furthermore, several studies have reported that the QAA model for IOPs has greater uncertainties in turbid inland waters (Jiang et al., 2019; Shanmugam et al., 2010) and it can be assumed those errors will be propagated to the estimations of $Kd_{(\lambda)}$ and Z_{SD}. Adopting recommendations that such semi-analytical algorithms designed for open ocean waters be modified before applying to coastal and inland waters (Huang et al., 2013) may further reduce retrieval uncertainties in the present study. Despite the extensive satellite matchups of a wide range of in situ Z_{SD} across diverse water types (oligotrophic through eutrophic, mineral turbidity through DOM-laden waters), the derived algorithm may still introduce uncertainties when applied to lakes outside of the validation dataset (here for example in Great Bear Lake and Lake Athabasca). While we believe the matchup dataset likely encompasses the water clarity properties of these two additional lakes, given what is known about their water conditions (oligotrophic in Great Bear and a gradient of turbid to oligotrophic in Athabasca), any future water quality monitoring on these under-sampled lakes would be valuable in further validating retrievals and assessing the broader transferability and uncertainties of the approach.

4.5. Management implications

Data scarcity remains a significant challenge in reporting on the status and long-term trends of inland water quality over countries as large as Canada and the U.S. with their vast water resources. For a Canada-wide assessment, Deutsch et al. (2022) reported on Secchi depth retrieved from Landsat 8 using a reflectance ratio algorithm for ~ 100,000 lakes across southern Canada, providing a valuable snapshot of the broad spatial patterns in water clarity in relation to lake morphological and hydrological conditions and human impacts. Here we provide a comprehensive assessment of the seasonal, interannual and decadal variability of water clarity for a number of Canada's large lakes, underscoring the significant temporal variability that the many lakes across Canada might experience. Such temporal time-series provide an effective indicator of lake responses to the cumulative impacts of hydroclimatic events, invasive species, eutrophication, and implemented water resource management actions. High fidelity remote sensing products made possible with merged multi-mission datasets will be critical for robust long-term monitoring and reporting of lake water quality status and trends, particularly in addressing directives of the newly formed Canada Water Agency and binational commitments for transboundary watersheds. Continuing efforts from space agencies and data providers to deliver consistent bias-minimized merged multi-mission data products would be welcome in reducing uncertainties in downstream products.

CRediT authorship contribution statement

Caren Binding: Writing – review & editing, Writing – original draft, Visualization, Validation, Project administration, Methodology, Investigation, Funding acquisition, Formal analysis, Data curation, Conceptualization. **Matt Morison:** Writing – review & editing, Data curation. **Michael Sayers:** Writing – review & editing, Data curation. **Karl Bosse:** Writing – review & editing, Data curation. **Xinhua Zhu:** Writing – review & editing, Data curation. **Chuiqing Zeng:** Writing – review & editing. **Varunan Theenathayalan:** Writing – review & editing.

Declaration of Competing Interest

The authors declare that they have no known competing financial interests or personal relationships that could have appeared to influence the work reported in this paper.

Acknowledgements

The authors wish to acknowledge Government of Canada funding under the Freshwater Action Plan. We thank the technical staff of Manitoba Environment and Climate Change, Lake Winnipeg Research Consortium Inc., the research vessels CCGS Limnos and M/V Namao, for their water quality surveillance data collection. We acknowledge also the following publicly available datasets that were used in this study: Ocean Colour Climate Change Initiative dataset, Version 6, European Space Agency (accessed at: https://www.esa-oceancolour-cci.org/); Ontario provincial government water quality monitoring (accessed at: https://data.ontario.ca/dataset/water-chemistry-great-lakes-nearshore-areas and https://data.ontario.ca/dataset/georgian-bay-water-quality); U.S. Environmental Protection Agency Great Lakes monitoring data available through the Great Lakes Environmental Database (GLENDA) (accessed via the U.S. Environmental Protection Agency (EPA) Central Data Exchange (CDX) at https://cdx.epa.gov/); ECCC's Great Lakes Water Quality Monitoring and Surveillance data (accessed at: https://data-donnees.ec.gc.ca/data/substances/monitor/

great-lakes-water-quality-monitoring-and-aquatic-ecosystem-health-data/great-lakes-water-quality-monitoring-and-surveillance-data/); and NOAA GLERL's HAB Monitoring program data available from the NOAA National Centers for Environmental Information (NCEI) at https://www.ncei.noaa.gov/.

Appendix A. Supplementary data

Supplementary data to this article can be found online at https://doi.org/10.1016/j.jglr.2024.102454.

References

Barbiero, R.P., Lesht, B.M., Warren, G.J., 2012. Convergence of trophic state and the lower food web in Lakes Huron, Michigan and Superior. J. Gt. Lakes Res. 38, 368–380. https://doi.org/10.1016/j.jglr.2012.03.009.

Barbiero, R.P., Tuchman, M.L., 2004. Long-term Dreissenid Impacts on Water Clarity in Lake Erie. J. Gt. Lakes Res. 30, 557–565. https://doi.org/10.1016/S0380-1330(04)70371-8.

Barbiero, R.P., Tuchman, M.L., Millard, E.S., 2006. Post-dreissenid Increases in Transparency During Summer Stratification in the Offshore Waters of Lake Ontario: Is a Reduction in Whiting Events the Cause? J. Gt. Lakes Res. 32, 131–141. https://doi.org/10.3394/0380-1330(2006)32[131:PIITDS]2.0.CO;2.

Binding, C.E., Jerome, J.H., Bukata, R.P., Booty, W.G., 2007. Trends in Water clarity of the lower great lakes from remotely sensed aquatic color. J. Gt. Lakes Res. 33, 828–841. https://doi.org/10.3394/0380-1330(2007)33[828:TIWCOT]2.0.CO;2.

Binding, C.E., Greenberg, T.A., Watson, S.B., Rastin, S., Gould, J., 2015. Long term water clarity changes in North America's Great Lakes from multi-sensor satellite observations. Limnol. Oceanogr. 60, 1976–1995. https://doi.org/10.1002/lno.10146.

Binding, C.E., Greenberg, T.A., McCullough, G., Watson, S.B., Page, E., 2018. An analysis of satellite-derived chlorophyll and algal bloom indices on Lake Winnipeg. J. Gt. Lakes Res. 44, 436–446. https://doi.org/10.1016/j.jglr.2018.04.001.

Binding, C.E., Zastepa, A., Zeng, C., 2019. The impact of phytoplankton community composition on optical properties and satellite observations of the 2017 western Lake Erie algal bloom. J. Gt. Lakes Res. 45, 573–586. https://doi.org/10.1016/j.jglr.2018.11.015.

Bunting, L., Leavitt, P.R., Simpson, G.L., Wissel, B., Laird, K.R., Cumming St., B.F., Amand, A., Engstrom, D.R., 2016. Increased variability and sudden ecosystem state change in Lake Winnipeg, Canada, caused by 20th century agriculture: Lake Winnipeg Variability and State Change. Limnol. Oceanogr. 61, 2090–2107. https://doi.org/10.1002/lno.10355.

CBC, 2020. Section of Great Slave Lake's water like "chocolate milk," boaters say.

Depew, D.C., Krutzelmann, E., Watchorn, K.E., Caskenette, A., Enders, E.C., 2021. The distribution, density, and biomass of the zebra mussel (Dreissena polymorpha) on natural substrates in Lake Winnipeg 2017–2019. J. Gt. Lakes Res. 47, 556–566. https://doi.org/10.1016/j.jglr.2020.12.005.

Deutsch, E.S., Fortin, M.-J., Cardille, J.A., 2022. Assessing the current water clarity status of ~100,000 lakes across southern Canada: A remote sensing approach. Sci. Total Environ. 20, 153971. https://doi.org/10.1016/j.scitotenv.2022.153971.

DFO, 2014. Lake Winnipeg zebra mussel treatment. DFO Canadian Science Advisory Secretary Science Response.

Dove, A., Chapra, S.C., 2015. Long-term trends of nutrients and trophic response variables for the Great Lakes: great Lakes nutrient trends. Limnol. Oceanogr. 60, 696–721. https://doi.org/10.1002/lno.10055.

ESA/ESRIN, 2022. Ocean Colour Climate Change Initiative (OC_CCI) – Phase 3, Product User Guide for v6.0 Dataset.

Evans, M., 2000. The large lake ecosystems of northern Canada. Aquat. Ecosyst. Health Manag. 3, 65–79.

Evans, M.A., Fahnenstiel, G., Scavia, D., 2011. Incidental oligotrophication of North American Great Lakes. Environ. Sci. Technol. 45, 3297–3303. https://doi.org/10.1021/es103892w.

Fahnenstiel, G., Nalepa, T., Pothoven, S., Carrick, H., Scavia, D., 2010. Lake Michigan lower food web: Long-term observations and Dreissena impact. Low. Food Web Lake Mich. Long-Term Trends Dreissenid Impact 36, 1–4. https://doi.org/10.1016/j.jglr.2010.05.009.

Gallegos, C.L., Correll, D.L., Pierce, J.W., 1990. Modeling spectral diffuse attenuation, absorption, and scattering coefficients in a turbid estuary. Limnol. Oceanogr. 35, 1486–1502. https://doi.org/10.4319/lo.1990.35.7.1486.

Government of Manitoba, 2020. A proposed Regulation under the Water Protection Act. Nutrient Concentration and Loading Targets for Lake Winnipeg and its Tributaries.

Government of Manitoba, 2023. Lake Winniepg: Nutrients and Loads Status Report 1994-2021, Manitoba Environment and Climate Report.

Groom, S., Sathyendranath, S., Ban, Y., Bernard, S., Brewin, R., Brotas, V., Brockmann, C., Chauhan, P., Choi, J., Chuprin, A., Ciavatta, S., Cipollini, P., Donlon, C., Franz, B., He, X., Hirata, T., Jackson, T., Kampel, M., Krasemann, H., Lavender, S., Pardo-Martinez, S., Mélin, F., Platt, T., Santoleri, R., Skakala, J., Schaeffer, B., Smith, M., Steinmetz, F., Valente, A., Wang, M., 2019. Satellite ocean colour: current status and future perspective. Front. Mar. Sci. 6, 485. https://doi.org/10.3389/fmars.2019.00485.

Hirsch, R.M., Slack, J.R., Smith, R.A., 1982. Techniques of trend analysis for monthly water quality data. Water Resour. Res. 18, 107–121. https://doi.org/10.1029/WR018i001p00107.

Ho, J.C., Michalak, A.M., Pahlevan, N., 2019. Widespread global increase in intense lake phytoplankton blooms since the 1980s. Nature 574, 667–670. https://doi.org/10.1038/s41586-019-1648-7.

Holland, R.E., 1993. Changes in Planktonic Diatoms and Water Transparency in Hatchery Bay, Bass Island Area, Western Lake Erie Since the Establishment of the Zebra Mussel. J. Gt. Lakes Res. 19, 617–624. https://doi.org/10.1016/S0380-1330(93)71245-9.

Huang, J., Chen, L., Chen, X., Song, Q., 2013. Validation of semi-analytical inversion models for inherent optical properties from ocean color in coastal Yellow Sea and East China Sea. J. Oceanogr. 69, 713–725. https://doi.org/10.1007/s10872-013-0202-8.

Huang, L., Timmermann, A., Lee, S.-S., Rodgers, K.B., Yamaguchi, R., Chung, E.-S., 2022. Emerging unprecedented lake ice loss in climate change projections. Nat. Commun. 13, 5798. https://doi.org/10.1038/s41467-022-33495-3.

Huot, Y., Brown, C.A., Potvin, G., Antoniades, D., Baulch, H.M., Beisner, B.E., Bélanger, S., Brazeau, S., Cabana, H., Cardille, J.A., del Giorgio, P.A., Gregory-Eaves, I., Fortin, M.-J., Lang, A.S., Laurion, I., Maranger, R., Prairie, Y.T., Rusak, J. A., Segura, P.A., Siron, R., Smol, J.P., Vinebrooke, R.D., Walsh, D.A., 2019. The NSERC Canadian Lake Pulse Network: a national assessment of lake health providing science for water management in a changing climate. Sci. Total Environ. 695, 133668. https://doi.org/10.1016/j.scitotenv.2019.133668.

Hussain, Md., Mahmud, I., 2019. pyMannKendall: a python package for non parametric Mann Kendall family of trend tests. J. Open Source Softw. 4, 1556. https://doi.org/10.21105/joss.01556.

IOCCG, 2007. Ocean-Colour Data Merging. In: Gregg, W. (Ed.), Reports of the International Ocean-Colour Coordinating Group, No. 6. IOCCG, Dartmouth, Canada.

Jerlov, N.G., 1976. Marine Optics. Elsevier.

Jiang, D., Matsushita, B., Setiawan, F., Vundo, A., 2019. An improved algorithm for estimating the Secchi disk depth from remote sensing data based on the new underwater visibility theory. ISPRS J. Photogramm. Remote Sens. 152, 13–23. https://doi.org/10.1016/j.isprsjprs.2019.04.002.

Keith, D.J., Salls, W., Schaeffer, B.A., Werdell, P.J., 2023. Assessing the suitability of lakes and reservoirs for recreation using Landsat 8. Environ. Monit. Assess. 195, 1353. https://doi.org/10.1007/s10661-023-11830-5.

Kerfoot, W.C., Yousef, F., Green, S.A., Budd, J.W., Schwab, D.J., Vanderploeg, H.A., 2010. Approaching storm: disappearing winter bloom in Lake Michigan. J. Gt. Lakes Res. 36, 30–41. https://doi.org/10.1016/j.jglr.2010.04.010.

Klerks, P.L., Fraleigh, P.C., Lawniczak, J.E., 1996. Effects of zebra mussels (Dreissena polymorpha) on seston levels and sediment deposition in western Lake Erie 53.

Lee, Z., Carder, K.L., Arnone, R.A., 2002. Deriving inherent optical properties from water color: a multiband quasi-analytical algorithm for optically deep waters. Appl. Opt. 41, 5755. https://doi.org/10.1364/AO.41.005755.

Lee, Z., Du, K., Arnone, R., 2005. A model for the diffuse attenuation coefficient of downwelling irradiance. J. Geophys. Res. Oceans 110. https://doi.org/10.1029/2004JC002275, 2004JC002275.

Lee, Z., Shang, S., Du, K., Wei, J., 2018. Resolving the long-standing puzzles about the observed Secchi depth relationships. Limnol. Oceanogr. 63, 2321–2336. https://doi.org/10.1002/lno.10940.

Lehmann, M.K., Gurlin, D., Pahlevan, N., Alikas, K., Conroy, T., Anstee, J., Balasubramanian, S.V., Barbosa, C.C.F., Binding, C., Bracher, A., Bresciani, M., Burtner, A., Cao, Z., Dekker, A.G., Di Vittorio, C., Drayson, N., Errera, R.M., Fernandez, V., Ficek, D., Fichot, C.G., Gege, P., Giardino, C., Gitelson, A.A., Greb, S. R., Henderson, H., Higa, H., Rahaghi, A.I., Jamet, C., Jiang, D., Jordan, T., Kangro, K., Kravitz, J.A., Kristoffersen, A.S., Kudela, R., Li, L., Ligi, M., Loisel, H., Lohrenz, S., Ma, R., Maciel, D.A., Malthus, T.J., Matsushita, B., Matthews, M., Minaudo, C., Mishra, D.R., Mishra, S., Moore, T., Moses, W.J., Nguyễn, H., Novo, E. M.L.M., Novoa, S., Odermatt, D., O'Donnell, D.M., Olmanson, L.G., Ondrusek, M., Oppelt, N., Ouillon, S., Pereira Filho, W., Plattner, S., Verdú, A.R., Salem, S.I., Schalles, J.F., Simis, S.G.H., Siswanto, E., Smith, B., Somlai-Schweiger, I., Soppa, M. A., Spyrakos, E., Tessin, E., van der Woerd, H.J., Vander Woude, A., Vandermeulen, R.A., Vantrepotte, V., Wernand, M.R., Werther, M., Young, K., Yue, L., 2023. GLORIA - A globally representative hyperspectral in situ dataset for optical sensing of water quality. Sci. Data 10, 100. https://doi.org/10.1038/s41597-023-01973-y.

Liu, J., Sun, D., Zhang, Y., Li, Y., 2013. Pre-classification improves relationships between water clarity, light attenuation, and suspended particulates in turbid inland waters. Hydrobiologia 711, 71–86. https://doi.org/10.1007/s10750-013-1462-4.

Maciel, D.A., Pahlevan, N., Barbosa, C.C.F., Martins, V.S., Smith, B., O'Shea, R.E., Balasubramanian, S.V., Saranathan, A.M., Novo, E.M.L.M., 2023. Towards global long-term water transparency products from the Landsat archive. Remote Sens. Environ. 299, 113889. https://doi.org/10.1016/j.rse.2023.113889.

Mélin, F., Vantrepotte, V., Chuprin, A., Grant, M., Jackson, T., Sathyendranath, S., 2017. Assessing the fitness-for-purpose of satellite multi-mission ocean color climate data records: a protocol applied to OC-CCI chlorophyll- a data. Remote Sens. Environ. 203, 139–151. https://doi.org/10.1016/j.rse.2017.03.039.

Messager, M.L., Lehner, B., Grill, G., Nedeva, I., Schmitt, O., 2016. Estimating the volume and age of water stored in global lakes using a geo-statistical approach. Nat. Commun. 7, 13603. https://doi.org/10.1038/ncomms13603.

Mood, A.M., 1950. Introduction to the Theory of Statistics.

Muir, A., Leonard, D.M., Krueger, C.C., 2013. Past, present and future of fishery management on one of the world's last remaining pristine great lakes: Great Bear Lake, Northwest Territories, Canada. Rev. Fish Biol. Fish. 23, 293–315. https://doi.org/10.1007/s11160-012-9295-1.

Nicholls, K.H., 2001. CUSUM phytoplankton and chlorophyll functions illustrate the apparent onset of Dreissenid Mussel impacts in Lake Ontario. J. Gt. Lakes Res. 27, 393–401. https://doi.org/10.1016/S0380-1330(01)70655-7.

Olmanson, L.G., Bauer, M.E., Brezonik, P.L., 2008. A 20-year Landsat water clarity census of Minnesota's 10,000 lakes. Remote Sens. Environ. 112, 4086–4097. https://doi.org/10.1016/j.rse.2007.12.013.

Page, E., 2020. Chapter 6: Lake Nutrient Concentrations, in: State of Lake Winnipeg, 2nd Edition. Environment and Climate Change Canada and Manitoba Agriculture and Reseource Development.

Cabin Radio, 2020. High water levels caused more sediment in Hay and Slave rivers.

Rao, Y.R., Huang, A., Schertzer, W.M., Rouse, W.R., 2012. Modelling of physical processes and assessment of climate change impacts in Great Bear Lake. Atmosphere-Ocean 50, 317–333. https://doi.org/10.1080/07055900.2012.668492.

Ruhland, K.M., Evans, M., Smol, J.P., 2023. Arctic warming drives striking twenty-first century ecosystem shifts in Great Slave Lake (Subarctic Canada), North America's deepest lake. Proc. Biol. Sci. 290, 20231252. https://doi.org/10.1098/rspb.2023.1252.

Sathyendranath, S., Brewin, R., Brockmann, C., Brotas, V., Calton, B., Chuprin, A., Cipollini, P., Couto, A., Dingle, J., Doerffer, R., Donlon, C., Dowell, M., Farman, A., Grant, M., Groom, S., Horseman, A., Jackson, T., Krasemann, H., Lavender, S., Martinez-Vicente, V., Mazeran, C., Mélin, F., Moore, T., Müller, D., Regner, P., Roy, S., Steele, C., Steinmetz, F., Swinton, J., Taberner, M., Thompson, A., Valente, A., Zühlke, M., Brando, V., Feng, H., Feldman, G., Franz, B., Frouin, R., Gould, R., Hooker, S., Kahru, M., Kratzer, S., Mitchell, B., Muller-Karger, F., Sosik, H., Voss, K., Werdell, J., Platt, T., 2019. An ocean-colour time series for use in climate studies: the experience of the Ocean-Colour Climate Change Initiative (OC-CCI). Sensors 19, 4285. https://doi.org/10.3390/s19194285.

Sayers, M., Bosse, K., Fahnenstiel, G., Shuchman, R., 2020. Carbon Fixation Trends in Eleven of the World's Largest Lakes: 2003–2018. Water 12, 3500. https://doi.org/10.3390/w12123500.

Scavia, D., David Allan, J., Arend, K.K., Bartell, S., Beletsky, D., Bosch, N.S., Brandt, S.B., Briland, R.D., Daloğlu, I., DePinto, J.V., Dolan, D.M., Evans, M.A., Farmer, T.M., Goto, D., Han, H., Höök, T.O., Knight, R., Ludsin, S.A., Mason, D., Michalak, A.M., Peter Richards, R., Roberts, J.J., Rucinski, D.K., Rutherford, E., Schwab, D.J., Sesterhenn, T.M., Zhang, H., Zhou, Y., 2014. Assessing and addressing the re-eutrophication of Lake Erie: Central basin hypoxia. J. Gt. Lakes Res. 40, 226–246. https://doi.org/10.1016/j.jglr.2014.02.004.

Shanmugam, P., Ahn, Y.-H., Ryu, J.-H., Sundarabalan, B., 2010. An evaluation of inversion models for retrieval of inherent optical properties from ocean color in coastal and open sea waters around Korea. J. Oceanogr. 66, 815–830. https://doi.org/10.1007/s10872-010-0066-0.

Stumpf, R.P., Wynne, T.T., Baker, D.B., Fahnenstiel, G.L., 2012. Interannual Variability of Cyanobacterial Blooms in Lake Erie. PLOS ONE 7, e42444.

Taranu, Z.E., Gregory-Eaves, I., Leavitt, P.R., Bunting, L., Buchaca, T., Catalan, J., Domaizon, I., Guilizzoni, P., Lami, A., McGowan, S., Moorhouse, H., Morabito, G., Pick, F.R., Stevenson, M.A., Thompson, P.L., Vinebrooke, R.D., 2015. Acceleration of cyanobacterial dominance in north temperate-subarctic lakes during the Anthropocene. Ecol. Lett. 18, 375–384. https://doi.org/10.1111/ele.12420.

Tong, Y., Feng, L., Wang, X., Pi, X., Xu, W., Woolway, R.I., 2023. Global lakes are warming slower than surface air temperature due to accelerated evaporation. Nat. Water 1, 929–940. https://doi.org/10.1038/s44221-023-00148-8.

USGS, 2020. Swirling Sediments in the Great Slave Lake. Earth Resources Observation and Science (EROS) Center.

van Oostende, M., Hieronymi, M., Krasemann, H., Baschek, B., Röttgers, R., 2022. Correction of inter-mission inconsistencies in merged ocean colour satellite data. Front. Remote Sens. 3, 882418. https://doi.org/10.3389/frsen.2022.882418.

Watkins, J.M., Rudstam, L.G., Crabtree, D.L., Walsh, M.G., 2013. Is reduced benthic flux related to the Diporeia decline? Analysis of spring blooms and whiting events in Lake Ontario. J. Gt. Lakes Res. 39, 395–403. https://doi.org/10.1016/j.jglr.2013.05.007.

Watson, S.B., Miller, C., Arhonditsis, G., Boyer, G.L., Carmichael, W., Charlton, M.N., Confesor, R., Depew, D.C., Höök, T.O., Ludsin, S.A., Matisoff, G., McElmurry, S.P., Murray, M.W., Peter Richards, R., Rao, Y.R., Steffen, M.M., Wilhelm, S.W., 2016. The re-eutrophication of Lake Erie: Harmful algal blooms and hypoxia. Harmful Algae 56, 44–66. https://doi.org/10.1016/j.hal.2016.04.010.

Williamson, C.E., Overholt, E.P., Pilla, R.M., Leach, T.H., Brentrup, J.A., Knoll, L.B., Mette, E.M., Moeller, R.E., 2015. Ecological consequences of long-term browning in lakes. Sci. Rep. 5, 18666. https://doi.org/10.1038/srep18666.

Zeng, C., Binding, C.E., 2021. Consistent multi-mission measures of inland water algal bloom spatial extent using MERIS, MODIS and OLCI. Remote Sens. 13, 3349. https://doi.org/10.3390/rs13173349.

Zhang, X., Hu, L., He, M.-X., 2009. Scattering by pure seawater: effect of salinity. Opt. Express 17, 5698. https://doi.org/10.1364/OE.17.005698.

Zhang, Y., Shi, K., Sun, X., Zhang, Y., Li, N., Wang, W., Zhou, Y., Zhi, W., Liu, M., Li, Y., Zhu, G., Qin, B., Jeppesen, E., Zhou, J., Li, H., 2022. Improving remote sensing estimation of Secchi disk depth for global lakes and reservoirs using machine learning methods. Giscience Remote Sens. 59, 1367–1383. https://doi.org/10.1080/15481603.2022.2116102.

Zhu, X., Chapelsky, A., Carmichael, T.J., Leonard, D.L., Lea, E., Tallman, R.F., Evans, M., Podemski, C., Low, G., 2017. Establishment of ecological baseline metrics for integrated ecomonitoring and assessment of cumulative impacts on Great Slave Lake fisheries ecosystems, Can. Tech. Rpt. Fish. Aquat. Sci. Fisheries and Oceans Canada, Fisheries and Oceans Canada, Winnipeg, Manitoba, Canada, [Ottawa].

Zhu, X., Leonard, D., Howland, K.J., VanGerwen-Toyne, M., Gallagher, C., Carmichael, T. J., Tallman, R.F., 2024. Fishery-Independent Gillnet Study (FIGS) sampling protocol used for multi-species ecology study in Great Slave Lake, Northwest Territories, Canada, CSAS Res. Doc. Canadian Science Advisory Secretariat (CSAS), Ottawa ON.